

# JFE980 S 高强钢激光—电弧复合热源 热模拟试验分析

王旭友， 滕 彬， 雷 振， 林尚扬  
(机械科学研究院哈尔滨焊接研究所， 哈尔滨 150080)

摘 要: 针对 JFE980 S 高强钢焊接热影响区的组织脆化、软化问题, 采用测温仪对激光—电弧复合焊和常规 MAG 焊两种焊接方法焊接热循环曲线进行测定, 通过测得的焊接热循环曲线, 利用 Gleeble3500 热力模拟试验机对这两种焊接方法热影响区的焊接过程进行模拟, 并对其组织、拉伸以及 -20℃ 冲击吸收功进行了分析和测试. 结果表明, 激光—电弧复合焊峰值温度停留时间和  $t_{8/5}$ 、 $t_{5/3}$  冷却时间均小于常规 MAG 焊; 模拟的焊接粗晶区冲击韧性是常规 MAG 焊的两倍, 不完全相变区拉伸性能比常规 MAG 焊提高了 100 MPa 以上.

关键词: 复合热源焊接; 热模拟; 脆化; 软化; 高强钢

中图分类号: TG115.28 文献标识码: A 文章编号: 0253-360X(2010)11-0025-04



王旭友

## 0 序 言

对于低合金高强钢的焊接, 主要存在焊接接头脆化、软化问题, 对于其研究工作多集中在一些传统的焊接方法上, 主要表现在热影响区的粗晶区 (1 000~1 300℃) 和不完全相变区 (700~800℃), 其中粗晶区主要表现为焊接接头性能的脆化, 而不完全相变区主要表现为焊接接头的软化问题<sup>[1-3]</sup>. 而利用激光—电弧复合热源焊接工艺在此方面的研究相对较少. 因此, 文中主要利用 JFE980 S 低合金调质高强钢, 采用热模拟方法分析激光—电弧复合焊和常规 MAG 焊接头抗脆化、软化的能力.

## 1 试验方法

试验所用低合金调质高强钢材质为 JFE980 S 钢, 钢板厚度为 12 mm, 焊材为  $\phi$ 1.2 HS-80 焊丝, 激光器为额定功率 2 kW 的连续波 Nd:YAG 激光器, 试验中采用焦距为 200 mm 的激光输出透镜; MAG/MIG 焊所用设备为 TPS000 型数字化电源. 母材和 HS-80 焊丝的化学成分见表 1, 母材力学性能见表 2. 所用热模拟试验机为 Gleeble3500 热力模拟试验机.

表 1 JFE980 S 钢及焊丝化学成分 (质量分数, %)  
Table 1 Chemical composition of JFE980 S and wire

|          | C    | Si   | Mn   | Cr   | Ni   | Mo   | Fe |
|----------|------|------|------|------|------|------|----|
| JFE980 S | 0.14 | 0.25 | 0.92 | 0.62 | 0.03 | 0.16 | 余量 |
| HS-80    | 0.09 | 0.55 | 1.68 | 0.02 | 1.02 | 0.43 | 余量 |

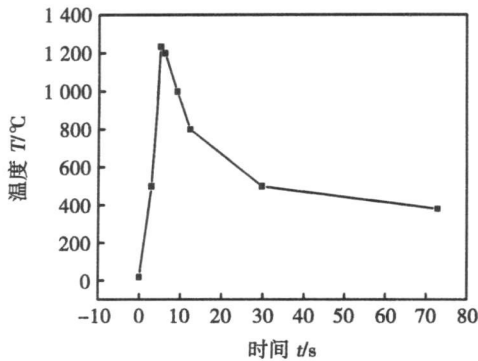
表 2 JFE980 S 钢板力学性能  
Table 2 Properties of JFE980 S

| 屈服强度<br>$R_{eL}/\text{MPa}$ | 抗拉强度<br>$R_m/\text{MPa}$ | 断后伸长率<br>$A(\%)$ | 冲击吸收功<br>$A_{KV(-20^\circ\text{C})}/\text{J}$ | 硬度<br>(HV) |
|-----------------------------|--------------------------|------------------|---|------------|
| 960                         | 1 005                    | 12.6             | >47   | 322        |

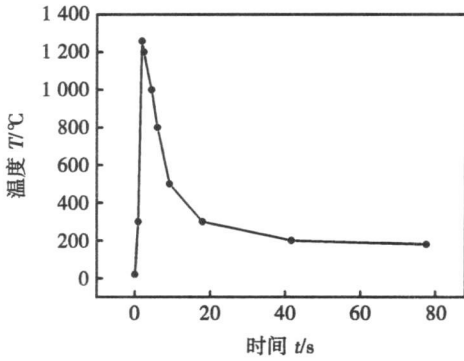
焊接热影响区的宽度很窄, 一般只有几毫米, 并在这几毫米的范围内包括有几个组织和性能不同的特定温度区. 若想在实际的焊接接头中, 对这些特定温度区的金属分别进行力学性能试验或可靠地测定焊接特性是困难的. 为了使焊接热影响区各特定部位的尺寸大到足以进行正常的性能试验, 只有采用焊接热模拟的方法才能达到.

焊接热模拟试验前, 对两种焊接方法进行了热循环曲线的测定. 首先对熔深进行测量, 根据测量的熔深在焊接试板背面钻取深度不同的盲孔, 盲孔内用储能点焊将测温仪的热电偶与试板相连接, 从而在焊接过程中利用测温仪采集不同深度的温度曲线, 从而获得热影响区不同部位的焊接热循环曲线. 焊接过程中常规 MAG 焊和激光复合焊热循环曲线

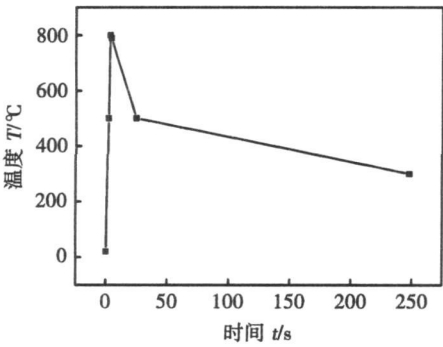
测定所用的焊接参数见表 3。经过测定两种焊接方法热循环曲线如图 1 所示。通过测得的热循环曲线对高强钢中容易出现脆化、软化的热影响区粗晶区



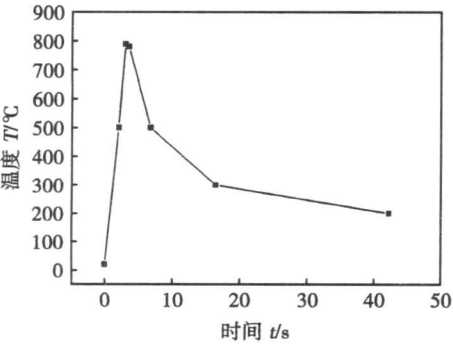
(a) 常规焊粗晶区



(b) 复合焊粗晶区



(c) 常规MAG焊不完全相变区



(d) 复合焊不完全相变区

图 1 两种焊接方法焊接热循环曲线

Fig 1 Welding thermal cycle curve of two kinds of welding method

表 3 焊接工艺参数  
Table 3 Welding parameters

|          | 焊接电流<br>I/A | 电弧电压<br>U/V | 焊接速度<br>$v/(mm \cdot min^{-1})$ | 激光功率<br>P/W |
|----------|-------------|-------------|---------------------------------|-------------|
| 复合焊      | 270         | 30          | 1 000                           | 1 200       |
| 常规 MAG 焊 | 270         | 30          | 330                             | —           |

和不完全相变区进行热模拟试验，进而分析激光复合焊和常规 MAG 焊在抵抗热影响区组织脆化、软化能力。

从图 1 热循环曲线中可见，与常规 MAG 焊相比，激光复合焊冷却速度快，峰值温度停留时间为 0.5 s， $t_{8/5}$  冷却时间为 3 s， $t_{5/3}$  冷却时间在 10 s 左右；而常规焊峰值温度停留时间为 1.0 s， $t_{8/5}$  冷却时间超过 20 s， $t_{5/3}$  冷却时间达到 200 s 以上。

2 试验结果与分析

图 2 与图 3 分别为在两种焊接方法热循环曲线模拟的粗晶区及不完全相变区金相组织形貌。从模拟的组织来看，与实际焊接接头的粗晶区及不完全相变区组织形态相同。

表 4 为模拟粗晶区 -20 °C 冲击吸收功，从数据中可见，模拟的激光复合焊冲击吸收功值高。造成冲击吸收功差别的原因是由于在两种热循环曲线下获得的金相组织不同。图 2 a、b 为模拟常规 MAG 焊粗晶区组织形貌，组织为粒状贝氏体；图 2 c、d 为模拟激光复合焊粗晶区组织，组织为板条马氏体。对于低合金高强度钢来说，获得板条马氏体组织能提高其强韧性能。正是由于模拟的激光复合焊获得的板条马氏体组织，因此冲击吸收功较高。另外，从晶粒度角度考虑，实际焊接接头常规焊及激光复合焊晶粒度为 3.5 级和 4 级，模拟的常规焊及激光复合焊晶粒度均为 3.5 级。晶粒度级别越高，晶粒越细，组织性能越好。从这点考虑，模拟的常规焊试件晶粒度与实际相比偏高，而模拟的激光复合焊试件晶粒度偏低，模拟的常规焊试件占有一定的优势，在强韧性方面应比实际情况略好。尽管如此，从表 4 中可见，模拟的常规 MAG 焊冲击吸收功仍没有模拟的激光复合焊冲击吸收功高。因此综合这两方面的优势，激光复合焊粗晶区抗脆性断裂的能力要高于常规 MAG 焊。

表 5 为模拟不完全相变区抗拉强度，从表 5 中可知，模拟的激光复合焊拉伸性能远远优于常规 MAG 焊性能。与母材的组织相比，不完全正火区的组织发生了明显的变化，母材的组织为均匀细小的回火索氏体，而不完全正火区的组织为回火索氏体 +

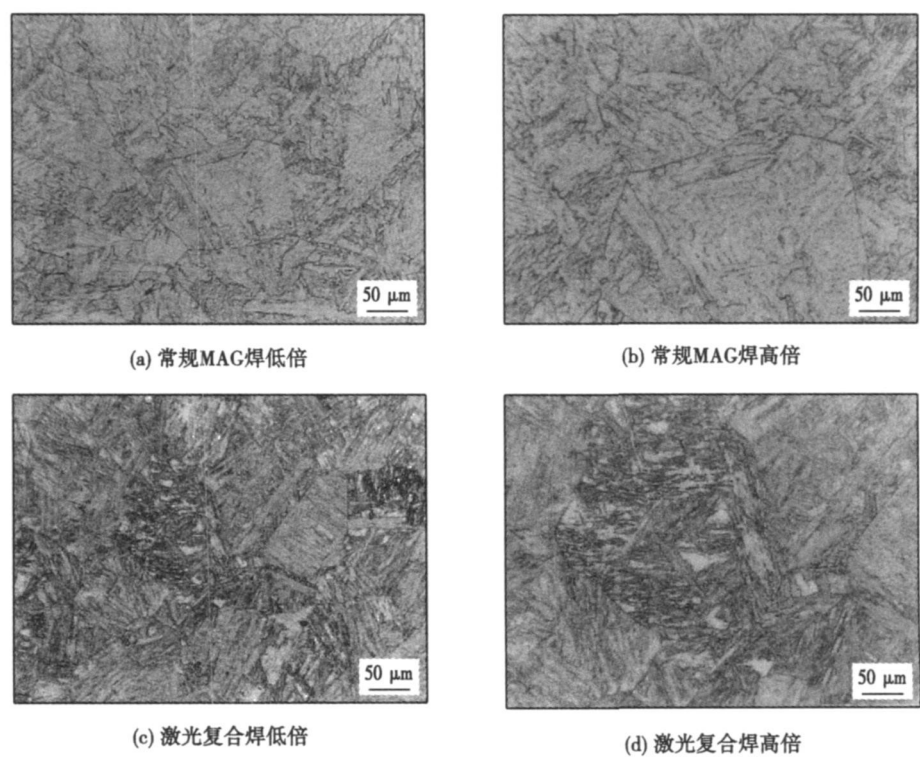


图 2 模拟粗晶区组织形貌  
Fig. 2 Microstructure of coarse grain zone by thermal simulation

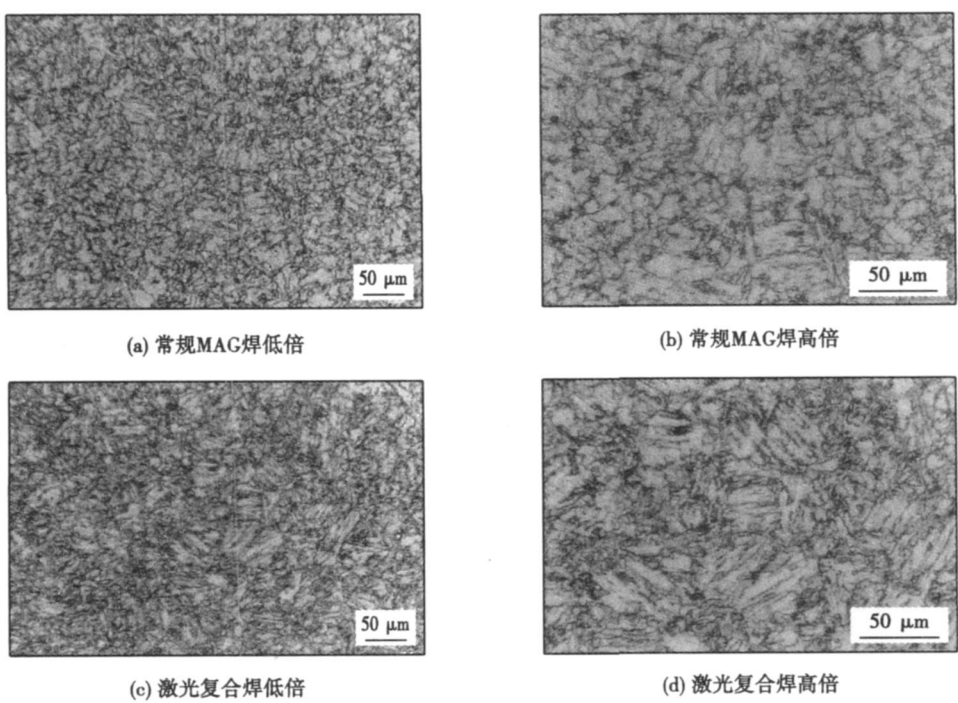


图 3 模拟不完全相变区组织形貌  
Fig. 3 Microstructure of incomplete phase transformation zone by thermal simulation

颗粒状或块状的马氏体 (或者是块状或颗粒状的碳化物 + 铁素体), 颗粒状或块状的马氏体主要分布在晶界附近. 这些在晶界附近呈颗粒状或块状分布

的马氏体组织改变了母材原回火索氏体组织的均匀性, 使得该区域的力学性能发生弱化, 便形成了焊接接头的软化区域. 尽管焊后激光—MAG复合热源

表 4 模拟粗晶区冲击吸收功

Table 4 Impact energy of coarse grain zone by thermal simulation

|     |    | 冲击吸收功 $A_{KV(-20\text{ }^{\circ}\text{C})}$ / J |    |    |    |
|-----|----|---|----|----|----|
| 常规焊 | 25 | 21  | 11 | 14 | 13 |
| 复合焊 | 24 | 38  | 38 | 34 | 44 |

焊接接头和常规 MAG 焊接头均出现了软化区域,但是从图 3 c、d 可以看出,与常规 MAG 焊区域组织相比,激光复合焊马氏体含量较多,在对模拟的不完全相变区进行显微硬度测试中发现,激光复合焊显微硬度为 344 HV<sub>0.1</sub>,常规 MAG 焊显微硬度为 266 HV<sub>0.1</sub>,可见激光复合焊软化效果较小。

表 5 模拟不完全相变区抗拉强度

Table 5 Tensile strength of incomplete phase transformation zone by thermal simulation

|     |     | 抗拉强度 $R_m$ / MPa |  |
|-----|-----|------------------|--|
| 常规焊 | 765 | 780              |  |
| 复合焊 | 910 | 890              |  |

与常规 MAG 焊相比,激光—电弧复合热源焊接方法高温停留时间,  $t_{8/5}$  和  $t_{5/3}$  冷却时间均小于前者。正是由于高温停留时间,冷却速度不同造成了激光复合焊焊接过程中抗接头脆化、软化的能力明显高于常规 MAG 焊。而两种焊接方法冷却不同归根结底是由于其激光复合焊和常规 MAG 焊本身工艺特点所决定。

3 结 论

(1) 通过模拟热影响区粗晶区组织,激光复合焊获得性能优异的板条马氏体组织,冲击吸收功明显高于常规 MAG 焊冲击性能,是常规 MAG 焊的两倍以上。

(2) 与母材相比,模拟激光复合焊和常规 MAG 焊不完全相变区组织发生了明显变化,从而造成焊接接头性能的弱化,但两者相比,常规 MAG 焊弱化效果更为显著,与激光复合焊相比,其常规焊模拟组织强度降低 100 MPa 以上。

(3) 造成激光复合焊和常规 MAG 焊热影响区组织性能差别主要是由于激光复合焊与常规 MAG 焊焊接过程的冷却速度不同。与常规 MAG 焊相比,激光复合焊高温停留时间短,冷却速度快,得到的组织均匀细小。

参考文献:

[ 1 ] 中国机械工程学会焊接学会. 焊接手册[ M ]. 2 卷. 北京: 机械工业出版社, 1992

[ 2 ] 李亚江, 邹曾大, 陈祝年, 等. 焊接热循环对 HQ130 钢焊接热影响区组织及性能的影响[ J ]. 金属学报, 1996 32( 5 ): 532—537  
Li Y a j i a n g , Z o u Z e n g d a , C h e n Z h u n j i a n , e t a l . E f f e c t s o f t h e w e l d t h e r m a l c y c l e o n m i c r o s t r u c t u r e a n d p r o p e r t i e s o f t h e h e a t a f f e c t e d z o n e o f H Q 1 3 0 s t e e l [ J ]. A c t a M e t a l l u r g i c a S i n i c a , 1 9 9 6 3 2 ( 5 ): 532—537

[ 3 ] 付瑞东, 逮允海, 杨永强, 等. 2 25Cr1Mo0. 25V 耐热钢焊接热影响区热模拟试验研究[ J ]. 材料热处理学报, 2007 28( 1 ): 66—70  
F u R u i d o n g , L u Y u n h a i , Y a n g Y o n g q i a n g . T h e r m a l s i m u l a t i o n e x p e r i m e n t s o f w e l d i n g h e a t a f f e c t e d z o n e o f 2 2 5 C r 1 M o 0 . 2 5 V h e a t r e s i s t a n c e s t e e l [ J ]. T r a n s a c t i o n s o f M a t e r i a l s a n d H e a t T r e a t m e n t , 2 0 0 7 2 8 ( 1 ): 6 6 — 7 0

作者简介: 王旭友, 男, 1965 年出生, 硕士, 研究员, 硕士研究生导师。主要从事激光加工和激光—电弧复合热源焊接技术方面的研究, 发表论文 10 余篇。

E m a i l : w a n g x u y o u @ t m . c o m

ingful. Furthermore, discussions about radial distributions of VPPA pressure can actually guide mechanical analysis and numerical simulation of VPPA and its molten pool. In this paper, the distribution of VPPA pressure along the radial distance at different welding currents was measured and discussed by U-tube barometer. It was concluded that the radial distribution of VPPA pressure still belonged to Gaussian distribution rather than exponential distribution. Furthermore, the analyzed results show that the VPPA pressure increases with the increase of welding current, but its increasing rate tends to slow.

**Key words:** variable polarity plasma arc welding; arc pressure; U-tube barometer; radial distribution

**Weld defect detection of double sides weld based on X-ray digitized image** SHAO Jiaxin, DU Dong, ZHU Xinjie, GAO Zhilong, WANG Chen (1. Key Laboratory for Advanced Materials Processing Technology, Ministry of Education, Tsinghua University, Beijing 100084, China; 2. North China Petroleum Steel Pipe Co., Ltd. Qingxian 062650, Hebei, China). P 21—24

**Abstract:** The automatic detection of weld defects based on image processing of X-ray digitized film is important in the engineering field. Ideas of respectively processing the weld edge area and the other area of weld and respectively processing the slim line defects and the other defects were proposed for automatic detection of the double sides weld defects. The outer edges and the edges of the overlapped area of double sides weld were segmented by grey waveform analysis with column by column. And then the large templates of median filter and mean filter were combined to simulate the weld background, and the weld defects were detected by segment threshold after the background being subtracted. The algorithms of adaptive image binarization with column by column and modified Hough transform were proposed to detect the slim line defects. The result shows that the proposed algorithm avoids false alarms on the edges of the overlapped area for the double sides weld and weak line defects are detected effectively.

**Key words:** X-ray inspection; double sides weld; weld defect; image processing

**Analysis on laser arc hybrid welded joint of high strength steel JFE980S by thermal simulation test** WANG Xuyou, TENG Bihai, LEI Zhen, LIN Shangyang (Harbin Welding Institute, China Academy of Machinery Science & Technology, Harbin 150080, China). P 25—28

**Abstract:** The brittlement and softening of HAZ of high strength steel JFE980S were studied by thermal simulation test. After the thermal cycle curve of laser hybrid welding and MAG welding being measured, the HAZ of two welding methods were simulated by means of the thermal simulation machine of Gleeble 3500, and the microstructure, tensile strength and the impact toughness at -20 °C of the specimens were tested and analyzed. The results indicate that the residence time of peak temperature,  $t_{8/5}$  and  $t_{5/3}$  in laser arc hybrid welding are all less than those in MAG welding. The impact toughness of the coarse grained region in joint by hybrid welding is as two times higher as that by MAG welding. The tensile strength of the incomplete

phase transformation region was increased by more than 100 MPa, which was compared with the common MAG welding.

**Key words:** hybrid welding; thermal simulation; brittlement; softening; high strength steel

**Ultrasonic welding mechanism of thermoplastics and its thermal process** ZHANG Zongbo, WANG Xiaodong, LUO Yi, ZHENG Yingsong, ZHANG Yanguo, WANG Lidong (1. Key Laboratory for Micro/Nano Technology and System of Liaoning Province, Dalian 116024, Liaoning, China; 2. Key Laboratory for Precision and Non-traditional Machining Technology of Ministry of Education, Dalian University of Technology, Dalian 116024, Liaoning, China). P 29—32

**Abstract:** Heat production mechanisms in temperature ranges below and above T<sub>g</sub> (glass transition temperature) of thermoplastic components were studied by numerical simulation and experiment. The viscoelastic heat and friction heat in ultrasonic welding of PMMA (polymethylmethacrylate) were numerically calculated by FEM (Finite Element Method). Temperature was measured to verify the simulation results. Results of simulation and experiment agree well with each other, which indicate that the friction heat is the initial heat source in ultrasonic welding process. Heat conduction effect chain reaction activates the generation of the viscoelastic heat when temperature reaches T<sub>g</sub> of the base metal. And the viscoelastic heat provides most required heat during welding. The present study gives a more clear understanding of heat production mechanisms in ultrasonic welding.

**Key words:** ultrasonic welding; viscoelastic heat; finite element method

**Analysis on joint softening for JFE980S high strength steel**

LEI Zhen, WANG Xuyou, TENG Bihai, ZHENG Hongyang (1. Harbin Welding Institute, China Academy of Machinery Science & Technology, Harbin 150080, China; 2. Heilongjiang Provincial Institute of Architectural Design and Research, Harbin 150008, China). P 33—37

**Abstract:** The softening problems in the joints of low alloy high strength steel JFE980S by laser/MAG hybrid welding and MAG welding were studied. The softening law and mechanism for the quenched and tempered low alloy high strength steel joints were discussed according to the results of tensile test, hardness test and microstructure analysis. The result indicated that the joints by MAG welding are seriously softened, but the joints by laser/MAG hybrid welding only are softened a little. And the softened zone width and the softened degree of the joints by laser/MAG hybrid welding are both smaller and lower than those of the joints by MAG welding. The softening mainly appears in over-tempering zone and incomplete normalizing zone in the HAZ. And the distribution of granular or nubby microstructure along the grain boundaries is the main reason of the softening.

**Key words:** quenched and tempered low alloy high strength steel; joint softening; laser/MAG arc hybrid welding

**Numerical simulation of keyhole formation process in laser**